Bending and buckling formulation of graphene sheets based on nonlocal simple first-order shear deformation theory

To cite this article: M E Golmakani *et al* 2018 *Mater. Res. Express* **5** 065010

Materials Research Express

PAPER

Bending and buckling formulation of graphene sheets based on nonlocal simple first-order shear deformation theory

RECEIVED
12 February 2018

REVISED
4 April 2018

ACCEPTED FOR PUBLICATION
21 May 2018

PUBLISHED
6 June 2018

M E Golmakani[1], M Malikan[1], M N Sadraee Far[1] and H R Majidi[2]

[1] Department of Mechanical Engineering, Mashhad Branch, Islamic Azad University, Mashhad, Iran
[2] Department of Mechanical Engineering, Iran University of Science and Technology (IUST), Narmak, 16846 Tehran, Iran

E-mail: m.e.golmakani@mshdiau.ac.ir

Keywords: large deflection, buckling, nonlocal elasticity theory, graphene sheets

Abstract

This paper presents a formulation based on simple first-order shear deformation theory (S-FSDT) for large deflection and buckling of orthotropic single-layered graphene sheets (SLGSs). The S-FSDT has many advantages compared to the classical plate theory (CPT) and conventional FSDT such as needless of shear correction factor, containing less number of unknowns than the existing FSDT and strong similarities with the CPT. Governing equations and boundary conditions are derived based on Hamilton's principle using the nonlocal differential constitutive relations of Eringen and von Kármán geometrical model. Numerical results are obtained using differential quadrature (DQ) method and the Newton–Raphson iterative scheme. Finally, some comparison studies are carried out to show the high accuracy and reliability of the present formulations compared to the nonlocal CPT and FSDT for different thicknesses, elastic foundations and nonlocal parameters.

1. Introduction

In recent years, nanostructures have been widely used in various engineering structures. One type of nanostructures with high usage is nanoplate which accurate prediction of its bending, vibrational and buckling behaviors becomes important and essential for engineering design and manufacturing. Nanoplates such as Graphene sheets (GSs) have attracted a great deal of attention from the researchers community for their superior properties and extensive applications in many fields such as modern aerospace, superfast biomedical, bioelectrical and nano-composites. Due to some disadvantages of experimental methods and atomistic simulation such as being difficult and expensive, various size dependent continuum theories such as nonlocal elasticity theory of Eringen have been widely applied to investigate the mechanical behaviors of carbon nanotubes and graphene sheets because of its simplicity, high consistency and good agreement with molecular dynamics (MD) simulations. In this way, several plate theories such as nonlocal first-order and higher-order shear deformation theories (FSDT) and (HSDTs) have been employed to study the mechanical behaviors of Graphene sheets [1–18]. The HSDTs can obtain higher accurate and stable solutions, but they require the continuity for the generalized displacements, and most importantly their computational costs are rather high. Also, the FSDT requires only inter element continuity but it suffers from the shear correction factor effects for thick plates [19]. Prabhu and Davalos [20] have derived a general expression for the shear correction factor of laminated rectangular beams and plates with arbitrary lay-up configurations using an energy equivalence principle. Their results indicate that value of 5/6 is desirable for the shear correction factor. But this amount is applicable for local one and cannot be suitable for nonlocal cases. Recently, Thai and Choi [21] proposed a simple first-order shear deformation theory (S-FSDT) for the bending and free vibration analysis of functionally graded plates to avoid the use of shear correction factors and reducing unknown parameters without reducing accuracy. In their method, the governing equations can be derived by partitioning the transverse deflection into the bending and shear components. Compared to the traditional FSDT, the S-FSDT is independent of shear correction factor and also one unknown can be saved by using this theory [19]. Up to now, some works have

been devoted to study the mechanical behavior of plates based on S-FSDT. Zenkour and Sobhy [22] studied a nonlocal simplified shear deformation plate theory for bending of nanobeams in thermal environment. They showed that results predicted by the S-FSDT are more accurate than those predicted by classical and shear deformation theories. Yu *et al* [19] investigated the R-FSDT for nonlinear bending analysis of functionally graded plates. Their results showed that deflections computed from the present method are in a good agreement with the other solutions. Yin *et al* [23] proposed a simple first-order shear deformation theory (S-FSDT) to consider the mechanical behavior of functionally graded plates. They found that S-FSDT method can be implemented by researchers within existing open-source isogeometric codes with very little effort and also, the S-FSDT based isogeometric analysis is well suited to the other solutions. Thai and Choi [24] studied the bending of laminated composite plates based on S-FSDT. Their studies show that results obtained by S-FSDT have the same accuracy with traditional FSDT which has more number of unknowns. Senjanovic *et al* [25] presented the consistent first-order shear deformation plate theory to consider shear-locking problem. Senjanovic *et al* [26] present a new beam theory to study the flexural and in-plane shear vibrations. Mantari and Granados [27] studied dynamic analysis of functionally graded plates using a novel FSDT with four unknowns. They used Navier's solution to solve the governing equations which were derived by employing the Hamilton's principle. Thai *et al* [28] derived a new simple four-unknown shear and normal deformations theory for static, dynamic and buckling analyses of isotropic and sandwich functionally graded (FG) plates.

According to the best of the author's knowledge, there is still no literature dealing with nonlocal formulations for nonlinear bending and buckling of orthotropic graphene sheets based on S-FSDT. Using the principle of virtual work and nonlocal differential constitutive relations of Eringen, the equilibrium equations of the nanoplate are derived in terms of the generalized displacements based on S-FSDT and the von Kármán nonlinear strains. Differential quadrature method is then used to solve some case studies for bending behavior of graphene sheets with simply-supported boundary condition. To verify the present results and formulations, some comparison studies are carried out between the obtained results and the conventional FSDT and classical plate theory (CPT) in the literature. The excellent agreement between the S-FSDT and those of FSDT and CPT shows the advantage of S-FSDT. Finally, some parametric studies have been carried out based on S-FSDT and conventional FSDT for bending behavior of nanoplates through considering various parameters such as small-scale parameter, thickness and elastic foundation.

2. Nonlocal bending formulation

Consider a rectangular nanoplate with length L_x, width L_y and thickness h as shown in figure 1. The displacement field according to the FSDT can be expressed by [2].

$$\begin{cases} u(x\ ,\ y\ ,\ z,\ t) = u_0(x,\ y,\ t) + z\varphi_x(x,\ y,\ t) \\ v(x\ ,\ y\ ,\ z,\ t) = v_0(x,\ y,\ t) + z\varphi_y(x,\ y,\ t) \\ w(x\ ,\ y\ ,\ z,\ t) = w_0(x,\ y,\ t) \end{cases} \tag{1}$$

where u, v and w are the displacement components of point (x, y, z) along x, y and z directions, respectively. Also u_0, v_0 and w_0 are the displacement functions of the middle surface of the plate. Moreover, φ_x and φ_y are the rotational displacement about the y and x directions, respectively.

As shown in figure 2, the shear stress is assumed to be constant in the thickness direction based on FSDT which is not true.

In the S-FSDT theory, it is assumed that transverse displacement w is divided into the bending component w_b and the shear component w_s, which means that:

$$w = w(bending) + w(shear) \tag{2}$$

Also, the rotation variable in the S-FSDT is expressed in terms of the bending component only:

$$\begin{aligned} \psi &= -\frac{\partial w_b}{\partial y} \\ \varphi &= -\frac{\partial w_b}{\partial x} \end{aligned} \tag{3}$$

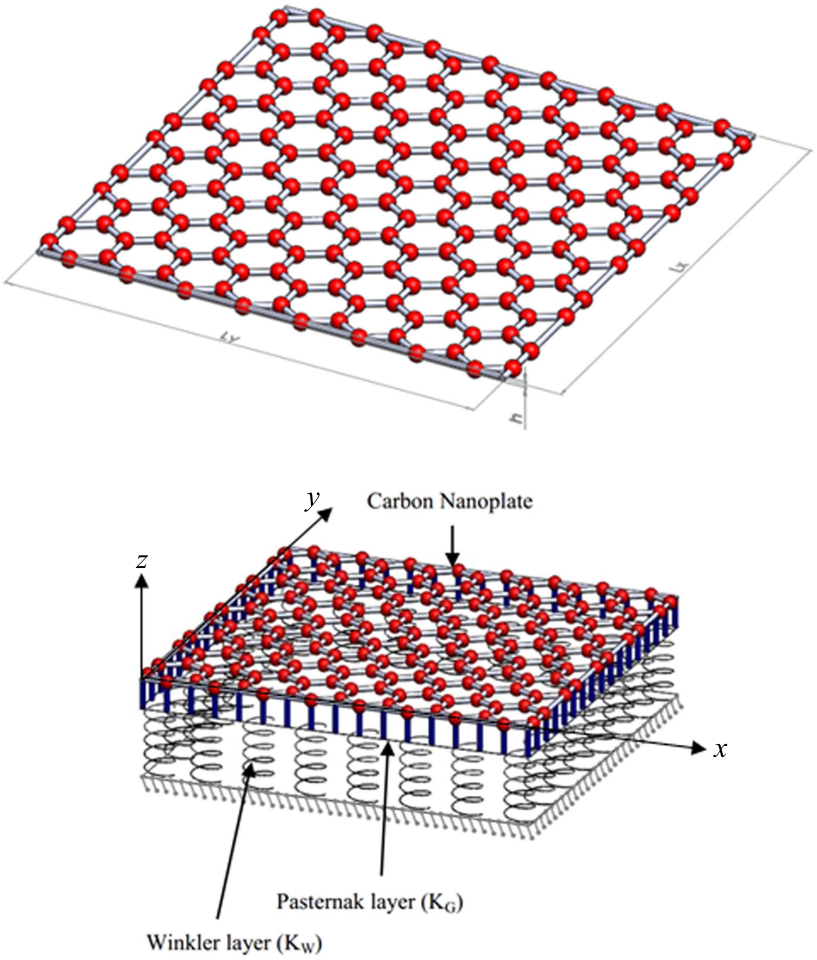

Figure 1. Geometry and coordinates of rectangular nanoplate on the polymer matrix.

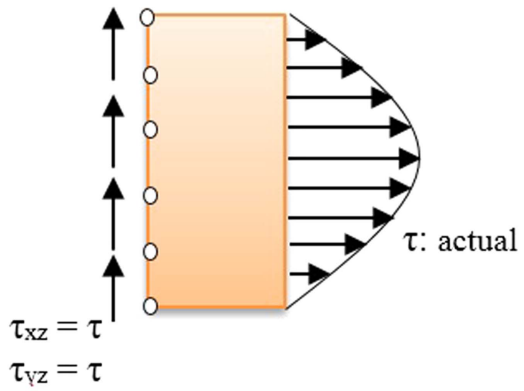

Figure 2. Shear stress in the thickness direction based on FSDT theory and actual state.

With implementation equations (2) and (3) into equation (1) it can be rewritten as follows:

$$\begin{cases} u(x\ ,\ y\ ,\ z,\ t) = u(x, y) - z\dfrac{\partial w_b}{\partial x} \\ v(x\ ,\ y\ ,\ z,\ t) = v(x, y) - z\dfrac{\partial w_b}{\partial y} \\ w(x, y, z) = w_b(x, y) + w_s(x, y) \end{cases} \tag{4}$$

The strains associated with the displacement field can be expressed by:

$$\varepsilon_{xx} = \frac{\partial u}{\partial x} - z\frac{\partial^2 w_b}{\partial x^2} + \frac{1}{2}\left(\frac{\partial w_b}{\partial x}\right)^2 + \frac{1}{2}\left(\frac{\partial w_s}{\partial x}\right)^2 + \frac{\partial w_b}{\partial x}\frac{\partial w_s}{\partial x}$$
$$\varepsilon_{yy} = \frac{\partial v}{\partial y} - z\frac{\partial^2 w_b}{\partial y^2} + \frac{1}{2}\left(\frac{\partial w_b}{\partial y}\right)^2 + \frac{1}{2}\left(\frac{\partial w_s}{\partial y}\right)^2 + \frac{\partial w_b}{\partial y}\frac{\partial w_s}{\partial y}$$
$$\gamma_{yz} = \frac{\partial w_s}{\partial y}, \quad \gamma_{xz} = \frac{\partial w_s}{\partial x}$$
$$\gamma_{xy} = \left(\frac{\partial u}{\partial y} + \frac{\partial v}{\partial x}\right) - 2z\frac{\partial^2 w_b}{\partial x \partial y} + \left(\frac{\partial w_b}{\partial x} + \frac{\partial w_s}{\partial x}\right)\left(\frac{\partial w_b}{\partial y} + \frac{\partial w_s}{\partial y}\right) \tag{5}$$

According to the nonlocal continuum theory of Eringen [29, 30] which accounts for small-scale effects, the stress at a reference point is defined by a function of the strain field at all neighbor points in the continuum body. The components of nonlocal stress tensor σ_{ij}(x) are given in the form of the following expression:

$$\sigma_{ij}(X) = \int \lambda(|X - X'|, \alpha)\tau_{ij}(X')\,dV(x') \quad \forall\, x \in V \tag{6}$$

Here, σ_{ij}, τ_{ij} are the nonlocal and classical or local stress tensors, respectively. $\lambda(|X - X'|, \alpha)$ is the nonlocal modulus function which describes the strain effect at X point for stress at reference point X', $|X - X'|$ denotes a Euclidean distance and V is the entire volume of body considered in this article. It can be observed that the integral constitutive relation (equation (6)) makes the elasticity problems difficult to solve. Therefore, the following differential form of the nonlocal constitutive equation is defined by Eringen [29, 31, 32].

$$(1 - \mu\nabla^2)\sigma^{nl} = \sigma^l \tag{7}$$

where $\mu = (e_0 a)^2$ is the nonlocal parameter which incorporates the small-scale effect $(e_0 a)$ into the formulation. It is noticed that e_0 is a value allocated to each material which is determined by matching the dispersion curves based on atomic models [29, 33], a is the internal characteristic length (like C–C bond length for carbon nanotube) and ∇^2 denotes the Laplacian operator and is given by $\nabla^2 = \partial^2/\partial x^2 + \partial^2/\partial y^2$. The hexagonal structure of graphene sheet leads to disparity between angles of in-plane load and inter-atomic bonds orientations at different directions [34].

The graphene sheets have anisotropic properties [35]. So, based on equation (7), the stress–strain equations of a rectangular orthotropic nanoplate can be expressed by the following generalized Hooke's law (subscript *nl* and *l* denote the quantities in nonlocal and local, respectively):

$$\begin{bmatrix}\sigma_{xx}\\ \sigma_{yy}\\ \sigma_{xy}\\ \sigma_{yz}\\ \sigma_{xz}\end{bmatrix}^{(nl)} - \mu\nabla^2\begin{bmatrix}\sigma_{xx}\\ \sigma_{yy}\\ \sigma_{xy}\\ \sigma_{yz}\\ \sigma_{xz}\end{bmatrix}^{(nl)} = [Q_{ijkl}] \times \begin{bmatrix}\varepsilon_{xx}\\ \varepsilon_{yy}\\ \varepsilon_{xy}\\ \varepsilon_{yz}\\ \varepsilon_{xz}\end{bmatrix}^{(l)} \tag{8}$$

In which:

$$[Q] = \begin{bmatrix} \frac{E_x}{1-\nu_{xy}\nu_{yx}} & \frac{\nu_{xy}Ey}{1-\nu_{xy}\nu_{yx}} & 0 & 0 & 0 \\ \frac{\nu_{yx}E_x}{1-\nu_{xy}\nu_{yx}} & \frac{E_y}{1-\nu_{xy}\nu_{yx}} & 0 & 0 & 0 \\ 0 & 0 & G_{yz} & 0 & 0 \\ 0 & 0 & 0 & G_{xz} & 0 \\ 0 & 0 & 0 & 0 & G_{xy} \end{bmatrix} \tag{9}$$

Also, moment and stress resultants of nonlocal elasticity are expressed as:

$$\begin{cases} (N_x,\ N_y,\ N_{xy},\ Q_x,\ Q_y) = \int_{-\frac{h}{2}}^{\frac{h}{2}} (\sigma_x,\ \sigma_y,\ \sigma_{xy},\ \sigma_{xz},\ \sigma_{yz})^{nl} dz \\ (M_x,\ M_y,\ M_{xy}) = \int_{-\frac{h}{2}}^{\frac{h}{2}} (\sigma_x,\ \sigma_y,\ \sigma_{xy})^{nl} z dz \end{cases} \tag{10}$$

Using equations (5), (8) and (10), the nonlocal stress resultants can be obtained in terms of displacements and rotations as follows:

$$\begin{bmatrix} N_{xx} \\ N_{yy} \\ N_{xy} \\ M_{xx} \\ M_{yy} \\ M_{xy} \\ Q_y \\ Q_x \end{bmatrix} - \mu\nabla^2 \begin{bmatrix} N_{xx} \\ N_{yy} \\ N_{xy} \\ M_{xx} \\ M_{yy} \\ M_{xy} \\ Q_y \\ Q_x \end{bmatrix} = \begin{bmatrix} A_{11} & A_{12} & 0 & 0 & 0 & 0 & 0 & 0 \\ A_{12} & A_{22} & 0 & 0 & 0 & 0 & 0 & 0 \\ 0 & 0 & A_{66} & 0 & 0 & 0 & 0 & 0 \\ 0 & 0 & 0 & D_{11} & D_{12} & 0 & 0 & 0 \\ 0 & 0 & 0 & D_{12} & D_{22} & 0 & 0 & 0 \\ 0 & 0 & 0 & 0 & 0 & D_{66} & 0 & 0 \\ 0 & 0 & 0 & 0 & 0 & 0 & H_{44} & 0 \\ 0 & 0 & 0 & 0 & 0 & 0 & 0 & H_{55} \end{bmatrix}$$
$$\times \begin{bmatrix} \frac{\partial u}{\partial x} + \frac{1}{2}\left(\frac{\partial w_b}{\partial x}\right)^2 + \frac{1}{2}\left(\frac{\partial w_s}{\partial x}\right)^2 + \frac{\partial w_b}{\partial x}\frac{\partial w_s}{\partial x} \\ \frac{\partial v}{\partial y} + \frac{1}{2}\left(\frac{\partial w_b}{\partial y}\right)^2 + \frac{1}{2}\left(\frac{\partial w_s}{\partial y}\right)^2 + \frac{\partial w_b}{\partial y}\frac{\partial w_s}{\partial y} \\ \frac{\partial u}{\partial y} + \frac{\partial v}{\partial x} + \left(\frac{\partial w_b}{\partial x} + \frac{\partial w_s}{\partial x}\right)\left(\frac{\partial w_b}{\partial y} + \frac{\partial w_s}{\partial y}\right) \\ -\frac{\partial^2 w_b}{\partial x^2} \\ -\frac{\partial^2 w_b}{\partial y^2} \\ -\frac{\partial^2 w_b}{\partial x \partial y} \\ \frac{\partial w_s}{\partial y} \\ \frac{\partial w_s}{\partial x} \end{bmatrix} \tag{11}$$

where $A_{ij}(i,j=1,2,6)$, $D_{ij}(i,j=1,2,6)$ and H_{44}, H_{55} are the extensional, bending and shear stiffness of the orthotropic sheets, respectively, defined by:

$$(A_{ij},\ D_{ij}) = \int_{-\frac{h}{2}}^{\frac{h}{2}} (1,\ z^2) Q_{ij}\, dz\ = \left(h,\ \frac{h^3}{12}\right) Q_{ij\ i,j=1,2,6}$$
$$H_{44} = G_{yz}h, \quad H_{55} = G_{xz}h \tag{12}$$

Using the Hamilton's principle, the governing equations as well as the related boundary conditions along the edges of rectangular graphene plate can be derived. The equations of the total potential energy are expressed as [14]:

$$\Pi = \int_0^t (\delta U + \delta\Omega)dt = 0 \tag{13}$$

In which U is strain energy and Ω is work done by external forces. In the case of static loading, the principle of virtual work can be expressed as follows based on nonlocal elasticity theory [36]:

$$\delta\Pi = \delta U + \delta\Omega_s + \delta\Omega_b = 0 \tag{14}$$

Here

$$\delta U = \iiint_V (\sigma_{xx}^{nl}\delta\varepsilon_{xx} + \sigma_{yy}^{nl}\delta\varepsilon_{yy} + \sigma_{xy}^{nl}\delta\varepsilon_{xy} + \sigma_{xz}^{nl}\delta\varepsilon_{xz} + \sigma_{yz}^{nl}\delta\varepsilon_{yz})dV \tag{15}$$

And, the works done by the external forces are defined by:

$$\delta\Omega_b = \int_0^{L_y}\int_0^{L_x} (q - k_W(w_b + w_s) + k_G\nabla^2(w_b + w_s))\delta w_b\, dxdy \tag{16}$$
$$\delta\Omega_s = \int_0^{L_y}\int_0^{L_x} (q - k_W(w_b + w_s) + k_G\nabla^2(w_b + w_s))\delta w_s\, dxdy$$

In which, k_W and k_G are Winkler and shear coefficients of foundation parameters, respectively. Furthermore, q indicates the uniform transverse load

Using the principle of stationary total potential energy, the nonlocal governing equations can be obtained. Then, by inserting equation (7) in nonlocal governing equations, the stress resultants in local forms are displayed in the following equations:

$$
\begin{aligned}
&N_{x,x} + N_{xy,y} = 0\\
&N_{xy,x} + N_{y,y} = 0\\
&\times Q_{x,x} + Q_{y,y} + (1 - \mu\nabla^2)N_{xx}\left(\frac{\partial^2 w_s}{\partial x^2} + \frac{\partial^2 w_b}{\partial x^2}\right) + (1 - \mu\nabla^2)N_{yy}\\
&\times \left(\frac{\partial^2 w_s}{\partial y^2} + \frac{\partial^2 w_b}{\partial y^2}\right) + 2(1 - \mu\nabla^2)N_{xy}\left(\frac{\partial^2 w_b}{\partial x\partial y} + \frac{\partial^2 w_s}{\partial x\partial y}\right)\\
&+ (1 - \mu\nabla^2)(q - k_W(w_b + w_s) + k_G\nabla^2(w_b + w_s)) = 0\\
&- M_{x,x} - 2M_{xy,y} - M_{y,y} + (1 - \mu\nabla^2)N_{xx}\left(\frac{\partial^2 w_s}{\partial x^2} + \frac{\partial^2 w_b}{\partial x^2}\right) + (1 - \mu\nabla^2)\\
&\times N_{yy}\left(\frac{\partial^2 w_s}{\partial y^2} + \frac{\partial^2 w_b}{\partial y^2}\right) + 2(1 - \mu\nabla^2)N_{xy}\left(\frac{\partial^2 w_b}{\partial x\partial y} + \frac{\partial^2 w_s}{\partial x\partial y}\right)\\
&+ (1 - \mu\nabla^2)(q - k_W(w_b + w_s) + k_G\nabla^2(w_b + w_s)) = 0
\end{aligned}
\tag{17}
$$

Using equations (11) and (17), the governing equations can be obtained in terms of the displacements. For the sake of brevity, only the first equation is given based on displacement field as follows:

$$
\begin{aligned}
&A_{11}\left(\frac{\partial^2 u}{\partial x^2} + \frac{\partial^2 w_b}{\partial x^2}\frac{\partial w_b}{\partial x} + \frac{\partial^2 w_s}{\partial x^2}\frac{\partial w_s}{\partial x} + \frac{\partial^2 w_b}{\partial x^2}\frac{\partial w_s}{\partial x} + \frac{\partial^2 w_s}{\partial x^2}\frac{\partial w_b}{\partial x}\right)\\
&+ A_{12}\left(\frac{\partial^2 v}{\partial x\partial y} + \frac{\partial^2 w_b}{\partial x\partial y}\frac{\partial w_b}{\partial y} + \frac{\partial^2 w_s}{\partial x\partial y}\frac{\partial w_s}{\partial y} + \frac{\partial^2 w_b}{\partial x\partial y}\frac{\partial w_s}{\partial y} + \frac{\partial^2 w_s}{\partial x\partial y}\frac{\partial w_b}{\partial y}\right)\\
&+ A_{66}\left(\frac{\partial^2 u}{\partial y^2} + \frac{\partial^2 v}{\partial x\partial y} + \frac{\partial^2 w_b}{\partial y^2}\frac{\partial w_b}{\partial x} + \frac{\partial w_b}{\partial y}\frac{\partial^2 w_b}{\partial x\partial y} + \frac{\partial^2 w_b}{\partial y^2}\frac{\partial w_s}{\partial x} + \frac{\partial w_b}{\partial y}\frac{\partial^2 w_s}{\partial x\partial y} + \frac{\partial^2 w_s}{\partial y^2}\frac{\partial w_b}{\partial x}\right.\\
&\left.+ \frac{\partial w_s}{\partial y}\frac{\partial^2 w_b}{\partial x\partial y} + \frac{\partial^2 w_s}{\partial y^2}\frac{\partial w_s}{\partial x} + \frac{\partial w_s}{\partial y}\frac{\partial^2 w_s}{\partial x\partial y}\right) = 0
\end{aligned}
\tag{18}
$$

3. Nonlocal buckling formulation

In this part, the single-layered graphene sheet (SLGS) resting on an elastic medium is simulated as a rectangular nanoplate. As seen in figure 1, the length, width and thickness of the sheet are defined by L_x, L_y and h, respectively, in x, y and z directions. Cartesian coordinate system is placed at one corner of the graphene sheet with the x, y and z axes along the length, width and thickness, respectively. Also, in-plane compressive loadings along the x and y axes are expressed by P_x and P_y, respectively, as follows:

$$P_x = P_y = P \tag{19}$$

To analyze the buckling behavior of graphene sheet, the stability equations are derived by the adjacent equilibrium criterion. According to this, the equilibrium equations are divided into pre-buckling and critical configurations in the following [16]:

$$
\begin{aligned}
N_{xx} &= N^0_{xx} + N^1_{xx}\\
N_{yy} &= N^0_{yy} + N^1_{yy}\\
N_{xy} &= N^0_{xy} + N^1_{xy}\\
M_{xx} &= M^0_{xx} + M^1_{xx}\\
M_{yy} &= M^0_{yy} + M^1_{yy}\\
M_{xy} &= M^0_{xy} + M^1_{xy}
\end{aligned}
\tag{20}
$$

In which:

$$
\begin{aligned}
&N^0_{x,x} + N^0_{xy,y} + N^1_{x,x} + N^1_{xy,y} = 0\\
&N^0_{xy,x} + N^0_{y,y} + N^1_{xy,x} + N^1_{y,y} = 0
\end{aligned}
\tag{21}
$$

Using the adjacent equilibrium criterion [16], the stability equations of mechanical buckling load can be expressed based on S-FSDT as follows:

$$N^1_{x,x} + N^1_{xy,y} = 0$$
$$N^1_{xy,x} + N^1_{y,y} = 0$$
$$-M^1_{x,x} - 2M^1_{xy,y} - M^1_{y,y} + (1-\mu\nabla^2)(P)\left(\frac{\partial^2 w^1_s}{\partial x^2} + \frac{\partial^2 w^1_b}{\partial x^2}\right) + (1-\mu\nabla^2)(P)\left(\frac{\partial^2 w^1_s}{\partial y^2} + \frac{\partial^2 w^1_b}{\partial y^2}\right)$$
$$+ (1-\mu\nabla^2)(-k_W(w^1_b + w^1_s) + k_G\nabla^2(w^1_b + w^1_s)) = 0$$
$$\times Q^1_{x,x} + Q^1_{y,y} + (1-\mu\nabla^2)(P)\left(\frac{\partial^2 w^1_s}{\partial x^2} + \frac{\partial^2 w^1_b}{\partial x^2}\right) + (1-\mu\nabla^2)(P)\left(\frac{\partial^2 w^1_s}{\partial y^2} + \frac{\partial^2 w^1_b}{\partial y^2}\right)$$
$$+ (1-\mu\nabla^2)(-k_W(w^1_b + w^1_s) + k_G\nabla^2(w^1_b + w^1_s)) = 0 \tag{22}$$

The stability equations can be expressed based on displacement components in the following equations:

$$A_{11}\left(\frac{\partial^2 u^1}{\partial x^2} + \frac{\partial^2 w^1_b}{\partial x^2}\frac{\partial w^1_b}{\partial x} + \frac{\partial^2 w^1_s}{\partial x^2}\frac{\partial w^1_s}{\partial x} + \frac{\partial^2 w^1_b}{\partial x^2}\frac{\partial w^1_s}{\partial x} + \frac{\partial^2 w^1_s}{\partial x^2}\frac{\partial w^1_b}{\partial x}\right)$$
$$+ A_{12}\left(\frac{\partial^2 v^1}{\partial x\partial y} + \frac{\partial^2 w^1_b}{\partial x\partial y}\frac{\partial w^1_b}{\partial y} + \frac{\partial^2 w^1_s}{\partial x\partial y}\frac{\partial w^1_s}{\partial y} + \frac{\partial^2 w^1_b}{\partial x\partial y}\frac{\partial w^1_s}{\partial y} + \frac{\partial^2 w^1_s}{\partial x\partial y}\frac{\partial w^1_b}{\partial y}\right)$$
$$+ A_{66}\left(\frac{\partial^2 u^1}{\partial y^2} + \frac{\partial^2 v^1}{\partial x\partial y} + \frac{\partial^2 w^1_b}{\partial y^2}\frac{\partial w^1_b}{\partial x} + \frac{\partial w^1_b}{\partial y}\frac{\partial^2 w^1_b}{\partial x\partial y} + \frac{\partial^2 w^1_b}{\partial y^2}\frac{\partial w^1_s}{\partial x}\right.$$
$$\left. + \frac{\partial w^1_b}{\partial y}\frac{\partial^2 w^1_s}{\partial x\partial y} + \frac{\partial^2 w^1_s}{\partial y^2}\frac{\partial w^1_b}{\partial x} + \frac{\partial w^1_s}{\partial y}\frac{\partial^2 w^1_b}{\partial x\partial y} + \frac{\partial^2 w^1_s}{\partial y^2}\frac{\partial w^1_s}{\partial x} + \frac{\partial w^1_s}{\partial y}\frac{\partial^2 w^1_s}{\partial x\partial y}\right) = 0 \tag{23}$$

$$A_{22}\left(\frac{\partial^2 v^1}{\partial y^2} + \frac{\partial^2 w^1_b}{\partial y^2}\frac{\partial w^1_b}{\partial y} + \frac{\partial^2 w^1_s}{\partial y^2}\frac{\partial w^1_s}{\partial y} + \frac{\partial^2 w^1_b}{\partial y^2}\frac{\partial w^1_s}{\partial y} + \frac{\partial^2 w^1_s}{\partial y^2}\frac{\partial w^1_b}{\partial y}\right)$$
$$+ A_{12}\left(\frac{\partial^2 v^1}{\partial x\partial y} + \frac{\partial^2 w^1_b}{\partial x\partial y}\frac{\partial w^1_b}{\partial x} + \frac{\partial^2 w^1_s}{\partial x\partial y}\frac{\partial w^1_s}{\partial x} + \frac{\partial^2 w^1_b}{\partial x\partial y}\frac{\partial w^1_s}{\partial x} + \frac{\partial^2 w^1_s}{\partial x\partial y}\frac{\partial w^1_b}{\partial x}\right)$$
$$+ A_{66}\left(\frac{\partial^2 u^1}{\partial x\partial y} + \frac{\partial^2 v^1}{\partial x^2} + \frac{\partial^2 w^1_b}{\partial x\partial y}\frac{\partial w^1_b}{\partial x} + \frac{\partial w^1_b}{\partial y}\frac{\partial^2 w^1_b}{\partial x^2} + \frac{\partial^2 w^1_b}{\partial x\partial y}\frac{\partial w^1_s}{\partial x} + \frac{\partial w^1_b}{\partial y}\frac{\partial^2 w^1_s}{\partial x^2}\right.$$
$$\left. + \frac{\partial^2 w^1_s}{\partial x\partial y}\frac{\partial w^1_b}{\partial x} + \frac{\partial w^1_s}{\partial y}\frac{\partial^2 w^1_b}{\partial x^2} + \frac{\partial^2 w^1_s}{\partial x\partial y}\frac{\partial w^1_s}{\partial x} + \frac{\partial w^1_s}{\partial y}\frac{\partial^2 w^1_s}{\partial x^2}\right) = 0 \tag{24}$$

$$H_{55}\frac{\partial^2 w^1_s}{\partial x^2} + H_{44}\frac{\partial^2 w^1_s}{\partial y^2} + (1-\mu\nabla^2)(P)\left(\frac{\partial^2 w^1_s}{\partial x^2} + \frac{\partial^2 w^1_b}{\partial x^2}\right) + (1-\mu\nabla^2)(P)\left(\frac{\partial^2 w^1_s}{\partial y^2} + \frac{\partial^2 w^1_b}{\partial y^2}\right)$$
$$+ (1-\mu\nabla^2)(-k_W(w^1_b + w^1_s) + k_G\nabla^2(w^1_b + w^1_s)) = 0 \tag{25}$$

$$D_{11}\frac{\partial^4 w^1_b}{\partial x^4} + 2(D_{12} + D_{66})\frac{\partial^4 w^1_b}{\partial x^2\partial y^2} + D_{22}\frac{\partial^4 w^1_b}{\partial y^4} + (1-\mu\nabla^2)(P)\left(\frac{\partial^2 w^1_s}{\partial x^2} + \frac{\partial^2 w^1_b}{\partial x^2}\right)$$
$$+ (1-\mu\nabla^2)(P)\left(\frac{\partial^2 w^1_s}{\partial y^2} + \frac{\partial^2 w^1_b}{\partial y^2}\right) + (1-\mu\nabla^2)(-k_W(w^1_b + w^1_s) + k_G\nabla^2(w^1_b + w^1_s)) = 0 \tag{26}$$

Here, two terms of N^1_{xx}, N^1_{yy} and small terms (order 2 and 3 related to w^1_b, w^1_s) are ignored for obtaining the final stability equations as follows:

$$(H_{55} + P)\frac{\partial^2 w^1_s}{\partial x^2} + (H_{44} + P)\frac{\partial^2 w^1_s}{\partial y^2} + P\left(\frac{\partial^2 w^1_b}{\partial x^2} + \frac{\partial^2 w^1_b}{\partial y^2}\right)$$
$$- \mu P\left(\frac{\partial^4 w^1_s}{\partial x^4} + \frac{\partial^4 w^1_s}{\partial y^4} + \frac{\partial^4 w^1_b}{\partial x^4} + \frac{\partial^4 w^1_b}{\partial y^4} + 2\frac{\partial^4 w^1_s}{\partial x^2\partial y^2} + 2\frac{\partial^4 w^1_b}{\partial x^2\partial y^2}\right)$$
$$+ (1-\mu)\left(-k_W\left(\frac{\partial^2 w^1_b}{\partial x^2} + \frac{\partial^2 w^1_b}{\partial y^2} + \frac{\partial^2 w^1_s}{\partial x^2} + \frac{\partial^2 w^1_s}{\partial y^2}\right)\right.$$
$$\left. + k_G\left(\frac{\partial^4 w^1_b}{\partial x^4} + \frac{\partial^4 w^1_s}{\partial x^4} + \frac{\partial^4 w^1_b}{\partial y^4} + \frac{\partial^4 w^1_s}{\partial y^4} + 2\frac{\partial^4 w^1_b}{\partial x^2\partial y^2} + 2\frac{\partial^4 w^1_s}{\partial x^2\partial y^2}\right)\right) = 0 \tag{27}$$

$$(D_{11} - \mu P)\frac{\partial^4 w_b^1}{\partial x^4} + (2(D_{12} + D_{66}) - 2\mu P)\frac{\partial^4 w_b^1}{\partial x^2 \partial y^2} + D_{22}\frac{\partial^4 w_b^1}{\partial y^4}$$
$$+ P\left(\frac{\partial^2 w_s^1}{\partial x^2} + \frac{\partial^2 w_s^1}{\partial y^2} + \frac{\partial^2 w_b^1}{\partial x^2} + \frac{\partial^2 w_b^1}{\partial y^2} - \mu\frac{\partial^4 w_s^1}{\partial x^4} - \mu\left(\frac{\partial^4 w_s^1}{\partial y^4} + \frac{\partial^4 w_b^1}{\partial y^4}\right) - 2\mu\frac{\partial^4 w_s^1}{\partial x^2 \partial y^2}\right)$$
$$+ (1 - \mu)\left(-k_W\left(\frac{\partial^2 w_b^1}{\partial x^2} + \frac{\partial^2 w_b^1}{\partial y^2} + \frac{\partial^2 w_s^1}{\partial x^2} + \frac{\partial^2 w_s^1}{\partial y^2}\right)\right.$$
$$\left. + k_G\left(\frac{\partial^4 w_b^1}{\partial x^4} + \frac{\partial^4 w_s^1}{\partial x^4} + \frac{\partial^4 w_b^1}{\partial y^4} + \frac{\partial^4 w_s^1}{\partial y^4} + 2\frac{\partial^4 w_b^1}{\partial x^2 \partial y^2} + 2\frac{\partial^4 w_s^1}{\partial x^2 \partial y^2}\right)\right) = 0 \tag{28}$$

4. Numerical methodology

To solve the equilibrium equations, differential quadrature method (DQM) [37] is employed in this study. In recent years, many researchers used DQM to analyze the nanostructures [38, 39]. DQM is an efficient numerical method for solving partial and ordinary differential equations. Based on the DQM, the partial derivative of a function with respect to a variable is estimated by considering a weighted linear sum of the functional values at all grid points in the whole domain. Therefore, the partial derivatives of a function $f(x, y)$ as an example, at the point (x_i, y_j) are expressed by [37]:

$$\frac{\partial^r f}{\partial x^r}(x_i, y_j) = \sum_{m=1}^{N} C_{im}^{(r)x} f(x_m, y_j) \quad i = 1, ...,N \tag{29}$$

$$\frac{\partial^r f}{\partial y^r}(x_i, y_j) = \sum_{r=1}^{M} C_{jr}^{(r)y} f(x_i, y_r) \quad j = 1, ...,M \tag{30}$$

where N and M are the number of grid points along x and y directions, respectively. Also, $C^{(r)x}$ and $C^{(r)y}$ are the weighting coefficients related to the sth-order derivative and for the first-order derivative ($r = 1$) can be obtained as follows [37]:

$$C_{ij}^{(1)x} = \begin{cases} \dfrac{R(x_i)}{(x_i - x_j)R(x_j)} & \text{for } i \neq j \\ \\ -\displaystyle\sum_{k=1, i\neq k}^{N} C_{ik}^{(1)x} & \text{for } i = j \end{cases} \qquad i,\ j = 1,\ 2, ..., N \tag{31}$$

$$C_{ij}^{(1)y} = \begin{cases} \dfrac{P(y_i)}{(y_i - y_j)P(y_j)} & \text{for } i \neq j \\ \\ -\displaystyle\sum_{k=1, i\neq k}^{M} C_{ik}^{(1)y} & \text{for } i = j \end{cases} \qquad i, j = 1,\ 2, ..., M \tag{32}$$

where $R(x_i)$ and $P(y_i)$ are defined by:

$$R(x_i) = \prod_{N}^{j=1} (x_i - x_j)\ i \neq j\ , \quad P(y_i) = \prod_{M}^{j=1} (y_i - y_j)\ i \neq j \tag{33}$$

Also, for higher-order partial derivatives ($r > 1$) the weighing coefficients along x and y directions are defined as follows:

$$C_{ij}^{(n)x} = \begin{cases} n\left[A_{ij}^{x} C_{ii}^{(n-1)x} - \dfrac{C_{ij}^{(n-1)x}}{(x_i - x_j)}\right] & \text{for } i \neq j \\ \\ -\displaystyle\sum_{j=1, \neq i}^{N} C_{ij}^{(n)x} & \text{for } i = j \end{cases} \qquad i, j = 1,\ 2, ...,N \tag{34}$$

Table 1. Comparison of the present results (S-FSDT) with those of [11, 14] and [37] for non-dimensional central deflection of the SLGS with simply-supported boundary condition.

	Non-dimensional central deflection			
q (psi)	FSDT [11]	FSDT [14]	CPT [37]	Present results
0.5	0.048	0.048	0.048	0.048
1.0	0.064	0.064	0.064	0.064
2.0	0.083	0.083	0.083	0.076
2.5	0.090	0.088	0.089	0.078
3.0	0.096	0.095	0.095	0.085

Table 2. Comparison between the non-dimensional central deflections of present results (S-FSDT) with those of [38] (CPT) and [14] (FSDT) for nonlocal bending analysis of simply-supported nanoplate.

	CPT [38]		FSDT [14]		Present results	
q(MPa)	$e_0a = 0.8$ nm	$e_0a = 0$ nm	$e_0a = 0.8$ nm	$e_0a = 0$ nm	$e_0a = 0.8$ nm	$e_0a = 0$ nm
20	0.1017	0.1105	0.0960	0.1037	0.0956	0.1035
40	0.1386	0.1526	0.1274	0.1382	0.1208	0.1377
60	0.1631	0.1789	0.1488	0.1609	0.1396	0.1544

$$\overline{C}_{ij}^{(m)y} = \begin{cases} m\left[A_{ij}^{y}\overline{C}_{ii}^{(m-1)y} - \dfrac{\overline{C}_{ij}^{(m-1)y}}{(y_i - y_j)}\right] & \text{for } i \neq j \\ & i, j = 1,\ 2, ...,M \\ -\sum\limits_{j=1,\neq i}^{M} \overline{C}_{ij}^{(m)y} & \text{for } i = j \end{cases} \tag{35}$$

In order to obtain the suitable number of discrete grid points and a better mesh point distribution, Chebyshev-Gauss-Lobatto technique has been employed as follows:

$$x_i = \frac{L_x}{2}\left(1 - \cos\left(\frac{i-1}{N-1}\right)\pi\right) \quad i = 1,\ 2, ...,N$$
$$y_j = \frac{L_y}{2}\left(1 - \cos\left(\frac{j-1}{M-1}\right)\pi\right) \quad j = 1,\ 2, ...,M \tag{36}$$

With implementation of DQM into the bending equations and also equations (27), (28), the discretized algebraic equations can be obtained. The mentioned set of nonlinear algebraic equations then will be solved using the Newton–Raphson method for bending analysis and also critical buckling load can be calculated using a standard eigenvalue solver.

5. Results and discussion

In order to verify the formulation, some comparison studies are carried out for large deflection behavior of the orthotropic single-layered graphene sheets (SLGSs) embedded in an elastic matrix based on FSDT, S-FSDT and CPT. The results are defined and presented in terms of the following dimensionless parameters:

$$W_1 = \frac{w_{b\,\max}}{L_x},\ K_G = \frac{k_G}{G_{xy} \times h},\ K_W = \frac{k_W \times {L_x}^2}{G_{xy} \times h} \tag{37}$$

To verify the present results in different values of thickness-to-length ratios, the current solutions for several thicknesses of nanoplates and nonlocal parameters are compared with those reported by [11, 14, 37, 38] for different transverse loads based on classical plate theory (CPT) and first-order shear deformation theory (FSDT). In order to achieve this goal, the SLGSs with different thickness values which are taken from [11, 14, 37, 38] is considered under simply-supported boundary conditions and uniform transverse load. As seen in tables 1 and 2, the FSDT and CPT results obtained by [11, 14, 37, 38] are in close agreement with the current solution. So, the reliability and accuracy of the present formulation with other reported results are verified. However, difference between the results of current theory and other plate theories increases with going up the load values of q which can be originated from shortcomings of CPT and FSDT in large deflections. As a matter of fact, in large

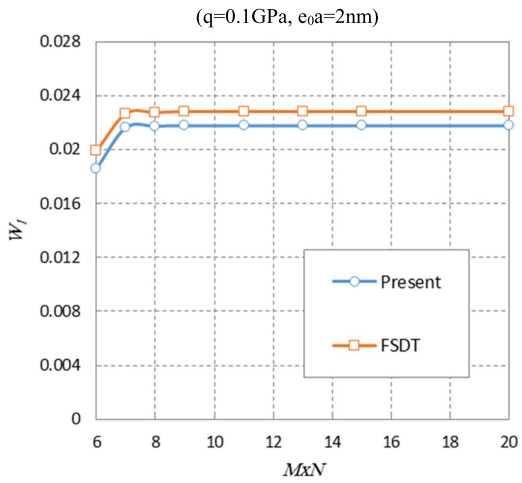

Figure 3. The convergence rate of the non-dimensional maximum deflections based on FSDT and S-FSDT.

deflections the error of assuming constant shear stress along the thickness in FSDT's assumptions will be further magnified. Furthermore, the influences of transverse shear strains which are ignored in CPT are more important in large deflections. Finally, regardless to the independency of S-FSDT to the shear correction coefficient, it should be noted that solving the governing equations based on S-FSDT is easier than the conventional FSDT owing to containing a smaller number of unknowns. The material properties and geometry of the SLGSs which are used in tables 1 and 2 are as follows:

Table 1: $E_x = 18.7e^6$, $E_y = 1.3e^6$, $G_{xy} = 0.6e^6$, $L_x = 9.4$ nm, $L_y = 7.75$ nm, $h = 0.0624$ nm, $\nu_{xy} = 0.3$ $\times$[11, 14, 37]

Table 2: $E_x = 2.434e^6$, $E_y = 2.473e^6$, $G_{xy} = 1.039e^6$, $L_x = 9.519$ nm, $L_y = 4.844$ nm, $h = 0.129$ nm, $\times \nu_{xy} = 0.197$[14, 38]

For more consideration between the present solution and those of conventional FSDT, the following material properties and dimensions have been used in bending analysis [15]:

$$L_x = L_y = 10.2 \text{ nm},\ h = 0.34 \text{ nm},\ E_x = 1765 \text{ GPa},\ E_y = 1588 \text{ GPa}$$
$$k_G = 1.13 \text{ Pa.m},\ \nu_{xy} = 0.3,\ \nu_{yx} = 0.27,\ k_W = 1.13 \text{ GPa.nm}^{-1} \quad (38)$$

In order to consider the effect of mesh size on the results, figure 3 reveals that if the grid points are based on 9 nodes in each coordinate direction, the results for deflections are converged to the identical values based on both nonlocal S-FSDT and FSDT. To this, all of the outcomes are obtained on the basis of the 9 $\times$ 9 nodes. Since in the DQ method the minimum numbers of nodes should be 3 $\times$ 3; therefore, before these nodes the value of deflection is zero and due to proximity of the results of FSDT and S-FSDT, the diagram is plotted after 6 $\times$ 6 grid point in order to further clarify of curves.

Furthermore, to investigate the discrepancy between the critical buckling load obtained by current solution and FSDT, some comparison and parametric studies have been carried out for the buckling analysis of the simply-supported orthotropic SLGS based on both S-FSDT and FSDT. In this way, the following dimensions and material properties have been considered [16]:

$$L_x = L_y = 10.77 \text{ nm},\ h = 0.34 \text{ nm},\ k_W = 1.13 \text{ GPa.nm}^{-1},\ k_G = 1.13 \text{ Pa.m},$$
$$E_x = 1765 \text{ GPa},\ E_y = 1588 \text{ GPa},\ \nu_{xy} = 0.3,\ \nu_{yx} = 0.27,\ k_s(FSDT) = 5/6 \quad (39)$$

In which k_s is transverse shear correction coefficient used for FSDT formulation to amend the effect of uniform transverse stress in shear forces.

Figure 4 shows the diagrams of non-dimensional central deflection (W_1) based on shear modulus of foundation for various values of small-scale parameter (e_0a) based on both FSDT and S-FSDT. As shown, with an increase in the shear modulus the deflection decreased slightly for both theories. By comparing FSDT and S-FSDT, it can be concluded that deflection obtained by S-FSDT is less than the results of FSDT. Also, by increasing the shear modulus of foundation the difference between responses of two theories decreased and the curves will be converged in higher values of shear modulus, especially in the small-scale effect of 2 nm.

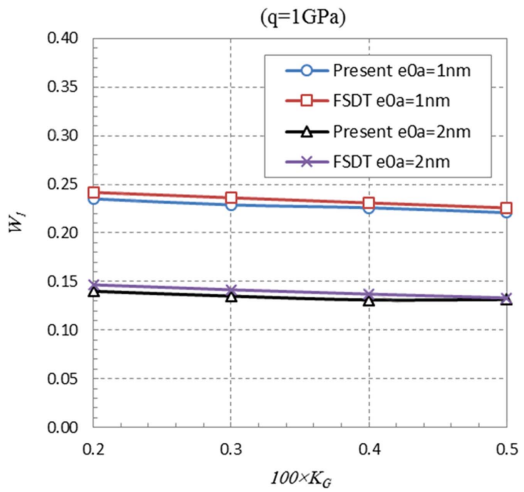

Figure 4. Effect of nondimensional Pasternak foundation parameter on non-dimensional central deflection for various small-scale values based on FSDT and S-FSDT.

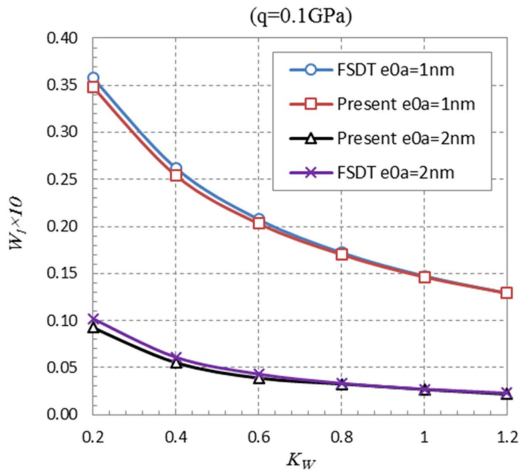

Figure 5. Effect of non-dimensional Winkler foundation parameter on dimensionless central deflection for different values of nonlocal parameter based on FSDT and S-FSDT.

Figure 5 illustrates the variations of non-dimensional central deflection in terms of dimensionless Winkler elastic foundation based on FSDT and S-FSDT. It is seen that with an increase in Winkler elastic foundation a nonlinear reduction of maximum deflection is observed in both types of theories. Furthermore, a comparison between two theories shows that when the non-dimensional Winkler elastic foundation increased to the point of 0.8 and further, the difference between FSDT and S-FSDT results declines and the results of two theories are in an excellent agreement in several values of nonlocal parameter.

Figures 6(a)–(c) demonstrate the non-dimensional central deflection in terms of thickness parameter for small-scale values of (a) $e_0a = 0$ nm, (b) $e_0a = 1$ nm and (c) $e_0a = 1.5$ nm based on FSDT and S-FSDT. A remarkable decrease is seen in non-dimensional maximum deflection as a result of increasing the plate thickness from 0.2 nm to 0.6 nm based on both theories. Also, with an increase in the thickness parameter the results of FSDT and S-FSDT will be converged and the convergence rate in the case of local theory is smaller than nonlocal one for both theories. A comparison of figures 6(a)–(c) indicates that with an increase in nonlocal parameter the difference between two theories increased. Furthermore, by increasing nonlocal parameter the convergence rate of curves goes up.

In order to show the difference of buckling load between the results of FSDT and S-FSDT for both uniaxial and biaxial loadings, figure 7 is presented in terms of small-scale value. As shown, there is a further difference in the results of uniaxial loading versus biaxial one in lower values of nonlocal factor. In addition, the critical buckling loads of uniaxial cases are significantly greater than those of biaxial case in $e_0a = 1$ nm, and the

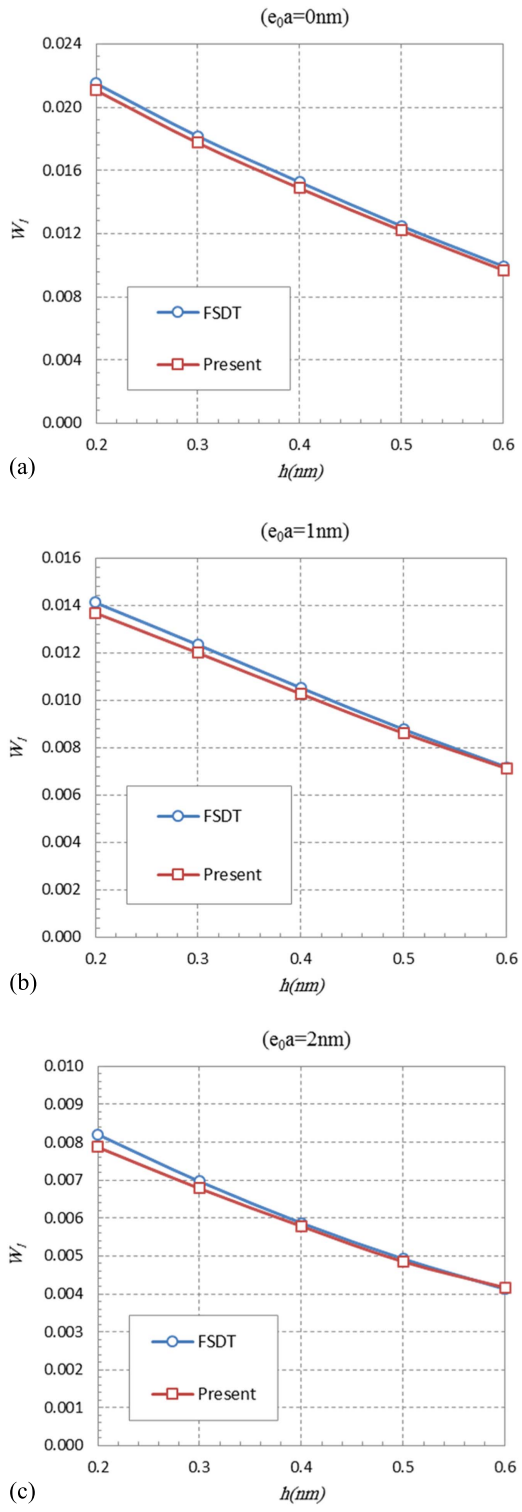

Figure 6. Diagram of non-dimensional central deflection based on thickness variable (q = 0.05 GPa) with different type of shear deformation theories for small-scale values of (a) e0a = 0 nm, (b) e_0a = 1 nm and (c) e_0a = 2 nm.

descending slope is also greater in the case of uniaxial analysis. It is worth noting that by an increase in small-scale parameter the results of uniaxial and biaxial cases are getting closer and closer to each other in both theories.

Figure 8 is presented to consider the effect of thickness-to-length ratio on the buckling load based on both S-FSDT and FSDT for two different values of nonlocal parameters. As illustrated, in a specified nonlocal parameter the differences between the buckling loads obtained by S-FSDT and FSDT goes up at higher values of thickness-to-length ratio. Also, in a definite thickness-to-length ratio the differences between the buckling loads

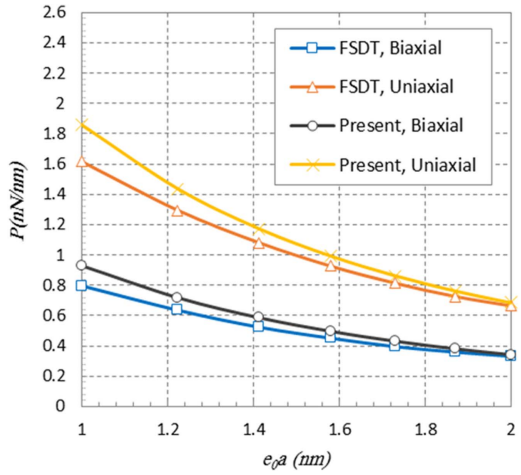

Figure 7. Uniaxial and biaxial critical buckling loads versus small-scale parameter based on S-FSDT and FSDT.

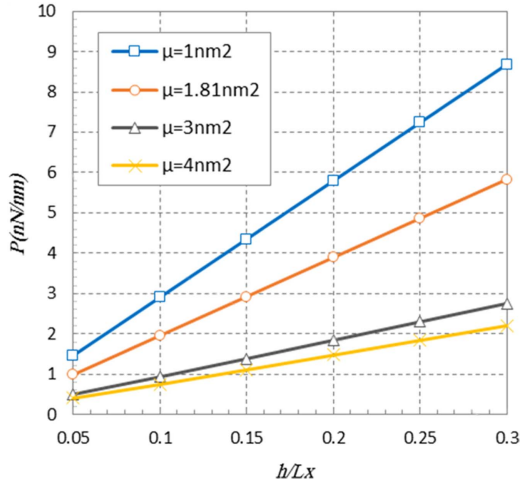

Figure 8. Influences of the ratio of thickness to length on the biaxial critical buckling loads for S-FSDT and FSDT theories.

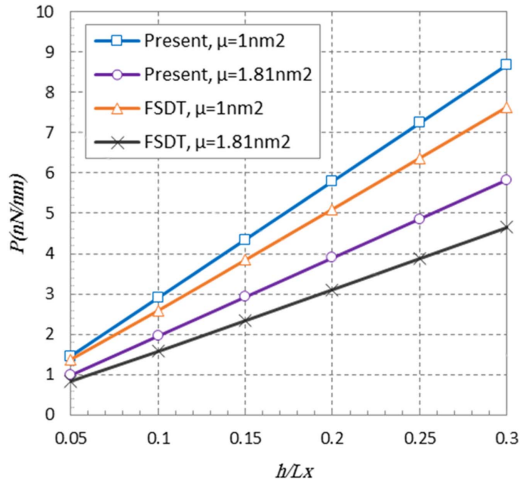

Figure 9. Influences of the ratio of thickness-to-length ratios for several small-scale parameters on the biaxial critical buckling loads.

determined by S-FSDT and FSDT increases in lower values of nonlocal parameter. Also, a significant increase in critical buckling loads is observed for plates having smaller nonlocal parameter.

Figure 9 shows the biaxial critical buckling loads of thin and moderately thick nanoplates for different values of the nonlocal parameter based on present theory. It can be seen from the figure that when the nonlocal parameter increased or when the plate becomes thicker, the slope of the critical buckling load curve increased more dramatically. It is also clear that with an increase in the thickness of the plate, the gap between the results obtained for various nonlocal parameter is getting larger at the same dimension ratio (h/L_x). In fact, the small-scale parameter has more effect on the buckling load for thicker plates.

6. Conclusions

In this work, the formulation of nonlinear bending and mechanical buckling of orthotropic SLGSs were presented based on S-FSDT. Using the Hamilton's principle, the equilibrium equations were obtained based on nonlocal elasticity theory and the von Kármán nonlinear strains. Differential quadrature method was used to solve the governing equation of these case studies. In order to consider the precision and advantage of new formulation, some comparison studies were conducted based on both FSDT and S-FSDT for bending and buckling analysis of graphene sheet through considering various parameters such as small-scale parameter, thickness and elastic foundation. Some general inferences are mentioned below:

- The S-FSDT formulation is free of the shear correction factor and number of unknowns and governing equations of the present FSDT are decline by one. So, this theory is efficient to use compared to the traditional FSDT.
- By comparing FSDT and S-FSDT solutions, deflections obtained by S-FSDT are less than FSDT ones and the critical buckling loads by S-FSDT are more than those of FSDT which result in this major conclusion that S-FSDT considered more stiffness for the SLGS compared to FSDT.
- Increase of plate thickness, Pasternak and Winkler elastic parameters play a decreasing role in the differences between S-FSDT and FSDT results in bending analysis.
- The difference between uniaxial buckling loads of FSDT with S-FSDT is more than biaxial ones, in particular in lower values of nonlocal parameter.
- By increasing the thickness of the plate the difference between buckling loads of S-FSDT and FSDT increased.

Compliance with ethical standards

The authors declare that they have no conflict of interest.

ORCID iDs

M E Golmakani https://orcid.org/0000-0002-0080-7168
M Malikan https://orcid.org/0000-0001-7356-2168
H R Majidi https://orcid.org/0000-0001-9602-9649

References

[1] Peddison J, Buchanan G R and McNitt R P 2003 Application of nonlocal continuum models nanotechnology *Int. J. Eng. Sci.* **41** 305–12
[2] Reddy J N 2010 Nonlocal nonlinear formulations for bending of classical and shear deformation theories of beams and plates *Int. J. Eng. Sci.* **48** 1507–18
[3] Aghababaei R and Reddy J N 2009 Nonlocal third-order shear deformation theory with application to bending and vibration of plates *J. Sound Vib.* **326** 277–89
[4] Pradhan S C 2009 Buckling of single layer graphene sheet based on nonlocal elasticity and higher order shear deformation theory *Physics Letters* A **373** 4182–8
[5] Samaei A T, Abbasian S and Mirsayar M M 2011 Buckling analysis of a single layer graphene sheet embedded in an elastic medium based on nonlocal Mindlin plate theory *Mech. Res. Commun.* **38** 481–5
[6] Malekzadeh P, Setoodeh A R and Alibeygi Beni A 2011 Small scale effect on the thermal buckling of orthotropic arbitrary straight-sided quadrilateral nanoplates embedded in an elastic medium *Compos. Struct.* **93** 2083–9
[7] Sarrami-Foroushani S and Azhari M 2013 Nonlocal vibration and buckling analysis of single and multi-layered graphene sheets using finite strip method including van der Waals effects *Physica* E **57** 83–95
[8] Bedroud M, Hosseini-Hashemi S and Nazemnezhad R 2013 Buckling of circular/annular Mindlin nanoplates via nonlocal elasticity *Acta Mech.* **224** 2663–76
[9] Xu Y M, Shen H S and Zhang C L 2013 Nonlocal plate model for nonlinear bending of bilayer graphene sheets subjected to transverse loads in thermal environments *Compos. Struct.* **98** 294–302

[10] Wang Y Z and Li F M 2012 Static bending behaviors of nanoplate embedded in elastic matrix with small scale effects *Mech. Res. Commun.* **41** 44–8
[11] Golmakani M E and Rezatalab J 2014 Nonlinear bending analysis of orthotropic nanoscale plates in an elastic matrix based on nonlocal continuum mechanics *Compos. Struct.* **111** 85–97
[12] Golmakani M E and Rezatalab J 2015 Nonuniform biaxial buckling of orthotropic nano plates embedded in an elastic medium based on nonlocal Mindlin plate theory *Compos. Struct.* **119** 238–50
[13] Ansari R, Mohammadi V, Faghih Shojaei M, Gholami R and Sahmani S 2014 Surface stress effect on the postbuckling and free vibrations of axisymmetric circular Mindlin nanoplates subject to various edge supports *Compos. Struct.* **112** 358–67
[14] Golmakani M E and Sadraee Far M N 2016 Nonlinear thermo-elastic bending behavior of graphene sheets embedded in an elastic medium based on nonlocal elasticity theory *Computers and Mathematics with Applications* **72** 785–805
[15] Golmakani M E and Sadraee Far M N 2017 Buckling analysis of biaxially compressed double-layered graphene sheets with various boundary conditions based on nonlocal elasticity theory *Microsyst. Technol.* **23** 2145–61
[16] Malikan M, Jabbarzadeh M and Dastjerdi S 2017 Non-linear static stability of bi-layer carbon nanosheets resting on an elastic matrix under various types of in-plane shearing loads in thermo-elasticity using nonlocal continuum *Microsyst. Technol.* **23** 2973–91
[17] Malikan M 2017 Electro-mechanical shear buckling of piezoelectric nanoplate using modified couple stress theory based on simplified first order shear deformation theory *Appl. Math. Modelling* **48** 196–207
[18] Malikan M 2018 Temperature influences on shear stability of a nanosize plate with piezoelectricity effect *Multidiscipline Modeling in Materials and Structures* **14** 125–42
[19] Tian T Y, Yin S, Bui T Q and Hirose S 2015 A simple FSDT-based isogeometric analysis for geometrically nonlinear analysis of functionally graded plates *Finite Elem. Anal. Des.* **96** 1–10
[20] Prabhu M-R and Davalos J F 1996 Static shear correction factor for laminated rectangular beams *Composites: Part* B **27** 285–93
[21] Thai H T and Choi D H 2013 A simple first-order shear deformation theory for the bending and free vibration analysis of functionally graded plates *Compos. Struct.* **101** 332–40
[22] Zenkour A M and Sobhy M 2015 A simplified shear and normal deformations nonlocal theory for bending of nanobeams in thermal environment *Physica* E **70** 121–8
[23] Yin S, Hale J S, Yu T, Bui T Q and Bordas S P A 2014 Isogeometric locking-free plate element: a simple first order shear deformation theory for functionally graded plates *Compos. Struct.* **118** 121–38
[24] Thai H T and Choi D H 2013 A simple first-order shear deformation theory for laminated composite plates *Compos. Struct.* **106** 754–63
[25] Senjanovic I, Vladimir N and Tomic M 2016 On new first-order shear deformation plate theories *Mech. Res. Commun.* **73** 31–8
[26] Senjanovic I, Vladimir N, Hadzic N and Tomic M 2016 New first order shear deformation beam theory with in-plane shear Influence *Engineering Structures.* **110** 169–83
[27] Mantari J L and Granados E V 2015 Dynamic analysis of functionally graded plates using a novel FSDT *Composites: Part* B **75** 148–55
[28] Thai C H, Zenkour A M, Wahab M A and Nguyen-Xuan H 2016 A simple four-unknown shear and normal deformations theory for functionally graded isotropic and sandwich plates based on isogeometric analysis *Compos. Struct.* **139** 77–95
[29] Eringen A C 2002 *Nonlocal Continuum Field Theories* (New York: Springer)
[30] Eringen A C 2006 Nonlocal continuum mechanics based on distributions *International Journal Engineering Science* **44** 141–7
[31] Fakher M and Hosseini Hashemi S 2017 Bending and free vibration analysis of nanobeams by differential and integral forms of nonlocal strain gradient with Rayleigh–Ritz method *Materials Research Express* **4** 125025
[32] Ebrahimi-Nejad S and Boreiry M 2018 Comprehensive nonlocal analysis of piezoelectric nanobeams with surface effects in bending, buckling and vibrations under magnetoelectro-thermo-mechanical loading *Materials Research Express* **5** 035028
[33] Eringen A C and Edelen D G B 1972 On nonlocal elasticity *International Journal Engineering Science* **10** 233–48
[34] Satish N, Narendar S and Gopalakrishnan S 2012 Thermal vibration analysis of orthotropic nanoplates based on nonlocal continuum mechanics *Physica* E **44** 1950–62
[35] Wang L and Zhang Q 2012 Elastic behavior of bilayer graphene under in-plane loadings *Current Application Physics* **12** 1173–7
[36] Hu H C 1984 *Variational Principles of Theory of Elasticity with Applications* (New York: Gordon and Breach)
[37] Chen W, Shu C, He W and Zhong T 2000 The application of special matrix product to differential quadrature solution of geometrically nonlinear bending of orthotropic rectangular plates *Comput. & Structures* **74** 65–76
[38] Shen H S, Shen L and Zhang C L 2011 Nonlocal plate model for nonlinear bending of single-layer graphene sheets subjected to transverse loads in thermal environments *Appl. Phys.* A **103** 103–12
[39] Shu C 2012 *Differential Quadrature and its Application in Engineering* (Berlin: Springer)